Leukemia
https://doi.org/10.1038/s41375-018-0065-5

ARTICLE

Immunotherapy

An "off-the-shelf" fratricide-resistant CAR-T for the treatment of T cell hematologic malignancies

Matthew L Cooper[1] · Jaebok Choi[1] · Karl Staser[1,2] · Julie K Ritchey[1] · Jessica M Devenport[1] · Kayla Eckardt[1] · Michael P Rettig[1] · Bing Wang[1] · Linda G Eissenberg[1] · Armin Ghobadi[1] · Leah N Gehrs[1] · Julie L Prior[3] · Samuel Achilefu[3] · Christopher A Miller[1,4] · Catrina C Fronick[4] · Julie O'Neal[1] · Feng Gao[5] · David M Weinstock[6] · Alejandro Gutierrez[6,7] · Robert S Fulton[4] · John F DiPersio[1]

Received: 18 December 2017 / Revised: 22 January 2018 / Accepted: 1 February 2018

Abstract

T cell malignancies represent a group of hematologic cancers with high rates of relapse and mortality in patients for whom no effective targeted therapies exist. The shared expression of target antigens between chimeric antigen receptor (CAR) T cells and malignant T cells has limited the development of CAR-T because of unintended CAR-T fratricide and an inability to harvest sufficient autologous T cells. Here, we describe a fratricide-resistant "off-the-shelf" CAR-T (or UCART7) that targets CD7+ T cell malignancies and, through CRISPR/Cas9 gene editing, lacks both CD7 and T cell receptor alpha chain (TRAC) expression. UCART7 demonstrates efficacy against human T cell acute lymphoblastic leukemia (T-ALL) cell lines and primary T-ALL in vitro and in vivo without the induction of xenogeneic GvHD. Fratricide-resistant, allo-tolerant "off-the-shelf" CAR-T represents a strategy for treatment of relapsed and refractory T-ALL and non-Hodgkin's T cell lymphoma without a requirement for autologous T cells.

Electronic supplementary material The online version of this article (https://doi.org/10.1038/s41375-018-0065-5) contains supplementary material, which is available to authorized users.

✉ Matthew L Cooper
matthewcooper@wustl.edu

✉ John F DiPersio
jdipersi@wustl.edu

[1] Department of Internal Medicine, Division of Oncology, Washington University School of Medicine, St. Louis, MO 63110, USA

[2] Department of Internal Medicine, Division of Dermatology, Washington University School of Medicine, St. Louis, MO 63110, USA

[3] Mallinckrodt Institute of Radiology, Washington University in St. Louis School of Medicine, St. Louis, MO 63110, USA

[4] McDonnell Genome Institute, Washington University School of Medicine, St. Louis, MO 63108, USA

[5] Department of Surgery, Division of Public Health Sciences, Washington University School of Medicine, St. Louis, MO 63110, USA

[6] Department of Medical Oncology, Dana-Farber Cancer Institute, Boston, MA 02215, USA

[7] Division of Hematology/Oncology, Boston Children's Hospital, Boston, MA 02215, USA

Introduction

T cell malignancies represent a class of hematologic cancers with high rates of relapse and mortality in both children and adults for which there are currently no effective or targeted therapies [1, 2]. Despite intensive multi-agent chemotherapy regimens, fewer than 50% of adults [3, 4] and 75% of children [5] with T-ALL survive beyond 5 years. For those who relapse after initial therapy, salvage chemotherapy regimens induce remissions in 20–40% of cases. Allogeneic stem cell transplant, with its associated risks and toxicities, is the only curative therapy [6].

T cells engineered to express a chimeric antigen receptor (CAR) are a promising cancer immunotherapy. Such targeted therapies have shown great potential for inducing both remissions and even long-term relapse free survival in patients with B cell leukemia and lymphoma [7–9]. Thus, clinically viable targeted therapy against T cell malignancies represents a significant unmet medical need. However, several challenges have limited the clinical development of CAR-T cells against T cell malignancies. First, the shared expression of target antigens between T effector cells and T cell malignancies results in fratricide, or self-killing, of CAR-T cells. Second, harvesting adequate numbers of autologous T cells, without contamination by malignant cells

Published online: 20 February 2018

is, at best, technically challenging and prohibitively expensive. Third, the use of genetically modified CAR-T cells from allogeneic donors may result in life-threatening graft-vs-host disease (GvHD) when infused into immune-compromised HLA-matched or mismatched recipients.

Many T cell malignancies express CD7, providing an attractive target for immunotherapy of T cell cancers [10–12]. However, normal T cells, including those used to engineer CAR-T, also express CD7 (>86%) [13]. Thus, CD7-targeted CAR-T cells induce T cell fratricide, limiting therapeutic potential. We hypothesized that deletion of CD7 and the T cell receptor alpha chain (TRAC) using CRISPR/Cas9 while also transducing these same T cells with a CD7 targeting CAR would result in the efficient targeting and killing of malignant T cells without significant effector T cell fratricide. TRAC deletion blocks TCR-mediated signaling, permitting the safe use of allogeneic T cells as the source of CAR-T without inducing life-threatening GvHD and without risk of contamination by CD7-deleted malignant cells, resistant to CART7 therapy. Using high-efficiency CRISPR/Cas9 gene editing, we generated CD7 and TRAC-deleted CAR-T targeting CD7 (UCART7). These UCART7 cells efficiently kill human T-ALL cell lines and patient-derived primary T-ALL in vitro and in vivo without resulting in xenogeneic GvHD. Accordingly, for the first time, we present preclinical data for an "off-the-shelf" strategy to effectively treat T cell malignancies using CAR-T therapy.

Materials and methods

CAR design

CD7-CAR was generated by using commercial gene synthesis of an anti-CD7 single-chain variable fragment (scFv) sequence found in patent WO2003051926_A2. The scFv was cloned into the backbone of a third-generation CAR with CD28 and 4-1BB internal signaling domains in the pELNS-Ef1α lentiviral vector (a kind gift from Dr. Carl June, University of Pennsylvania) [14]. The construct was modified to express the extracellular domain of hCD34 via a P2A peptide to enable both detection of CAR following viral transduction and, if required, purification of CAR-T using anti-hCD34 magnetic beads. Similarly, constructed CAR-T targeting CD19 were generated using an scFv obtained from Roguska et al. and were used as a non-targeting control [15].

Viral vector production

To produce lentivirus, the Lenti-X 293T Cell Line (Takara Bio, Mountain View, CA) was transfected with CAR lentiviral vector and the packaging plasmids, pMD.Lg/pRRE, pMD.G, pRSV.Rev [16, 17] using the CalPhos™ Mammalian Transfection Kit (Takara) per the manufacture's instructions. Virus was harvested 36 h post transfection, filtered to remove cell debris, and concentrated by ultracentrifugation for 90 min at 25,000 rpm, 4° C (Optima LE-80K Ultracentrifuge, Beckman Coulter, Indianapolis, IN). Virus was re-suspended in phosphate-buffered saline, snap frozen in liquid nitrogen and stored at −80 °C in single use aliquots.

CRISPR/cas9 gene editing

Guide RNA were designed and validated for activity by Washington University Genome Engineering & iPSC Center (Supplemental Table 1). Plasmids encoding gRNA (400 ng, Addgene 43860) and spCas9 (500 ng, Addgene 43945) were electroporated into the leukemia cell line, K562, using the nucleofector 4D (Lonza. NJ) in 20 µl solution P3 (program FF-120).

RNA guides were commercially synthesized (Trilink Biotechnologies San Diego, CA), incorporating 2′-*O*-methyl and 3′ phosphorothioate bases at the three terminal bases of the 5′ and 3′ ends of the gRNA to protect from nuclease activity [18]. Full guide sequences can be found in supplemental table 2. Streptococcus pyogenes Cas9 (spCas9) mRNA (5meC, Ψ) was purchased from Trilink Biotechnologies.

Gene-edited CAR-T

T cells were cultured in Xcyte media supplemented with 50 U/ml IL-2 and 10 ng/ml IL-15 in the presence of anti-CD3/CD28 beads (Bead to cell ratio 3:1). On day +2 post activation, beads were removed and 4×10^6 T cells were electroporated in 100 µl buffer P3 with 15 µg spCas9 (Trilink CA) and 20 µg of each gRNA (Trilink) using a nucleofector 4D, program EO-115. Cells were transduced with CAR7 or CAR19 (control) lentiviral particles in the presence of polybrene (Sigma-Aldrich. St. Louis, MO) (final conc. 6 µg/ml) on day +3. Cells were expanded for an additional 6 days prior to use in downstream experiments.

Targeted deep sequencing

The *CD7* locus was amplified with primers F_gcctgcgtgggatctacctgaggca and R_ AGCTATCTAGGAGGCTGCTGGGGGC. The *TRAC* locus was amplified with F_ TGGGGCAAAGAGGGAAATGA R_ GTCAGATTTGTTGCTCCAGGC. PCR products were sequenced using the Illumina MiSeq platform (San Diego, CA). Editing efficiencies were determined as a percentage of sequencing reads with indels aligned to reads obtained from WT cells.

Cell lines

CD7-positive T-ALL cell lines, MOLT-3 (ACC 84), MOLT-4 (ACC 362), HSB-2 (ACC 435), and CCRF-CEM (ACC 240) were obtained from directly from DSMZ-German collection of Microorganisms and Cell cultures (Leibniz, Germany). The cell lines were mycoplasma tested and characterized by DSMZ. CCRF-CEM cells were transduced with EF1α$^{CBR\text{-}GFP}$ lentivirus. GFP-positive cells were sorted and cloned to establish the CCRF-CEM$^{CBR\text{-}GFP}$ cell line.

Chromium release assay

CAR-T were incubated with MOLT-3, MOLT4, HSB-2, or CCRF cell lines (1×10^4 total cells/well) at an effector:target [E:T] ratio ranging from 25:1 to 0.25:1 in RPMI supplemented with 5% fetal calf serum. Chromium-51 release assays were performed as described previously [19].

In vitro primary T-ALL killing assay

Primary T-ALL from consented patients were obtained from the Siteman Cancer Center (IRB #201108251). Informed consent was obtained from all subjects. Primary cells were labeled with 150 nM carboxyfluorescein succinimidyl ester (CFSE) (Sigma-Aldrich, MO) to enable distinction between T-ALL blasts and CAR-T. Labeled cells were co-incubated at 1:1 ratio with either CD7$^{\Delta}$CART7, UCART7, or their respective CD19 controls for 24 h in Xcyte media supplemented with 50 U/mL IL-2 and 10 ng/ml IL-15, 50 ng/ml SCF, 10 ng/ml IL-7, and 20 ng/ml FL3TL prior to FACS analysis. Absolute cell counts of viable target cells were quantified by flow cytometry using 7-aminoactinomycin D and SPHERO AccuCount fluorospheres (Spherotech Inc., Lake Forest, IL, USA) as previously described [20]. Data were analyzed using FlowJo V10.

Fratricide assay

WT T cells were cultured in Xcyte media supplemented with 50 U/mL IL-2 and 10 ng/ml IL-15 in the presence of anti-CD3/CD28 beads (bead to cell ratio 3:1). Beads were removed after 48 h and T cell were transduced with lentivirus particles to express GFP. Seventy-two hours post transduction, T cells were sorted for GFP using flow cytometry and co-incubated with CD7$^{\Delta}$CART7 or CD7$^{\Delta}$CART19 at a ratio of 1:1 for 24 h in Xcyte media supplemented with 50 U/mL IL-2 and 10 ng/ml IL-15. Percent GFP+ cells were calculated as a percentage of total viable cells, quantified by flow cytometry using 7-aminoactinomycin D.

T cell phenotype analysis

Cultured T cells were washed in PBS/0.1% BSA and re-suspended at 1×10^6 cells in 50 µL Brilliant Buffer (BD Biosciences) supplemented with 4% rat serum for 15 min at 4 °C. Cells were then incubated for 30 min at 4 °C in 100 µL of Brilliant Buffer using the following antibody fluorophore conjugates (all from BD Biosciences unless otherwise noted): CD7 BV421, CD4 BV510, CCR4 BV605 (BioLegend), CD8 BV650, CD196 BV786 (BioLegend), CD3 AF488, CD45RA PerCPCy5.5, CD183 PE, CD197 PE-CF594, CD185 PE-Cy7 (BioLegend), and CCR10 APC (R&D Systems). Full details of fluorophore-conjugated antibodies can be found in Supplemental Table 5. Cells were then washed twice in PBS/0.1% BSA and data acquired on a ZE5 (Yeti) cytometer (BioRad/Propel Labs). Compensation and analyses were performed on FlowJo V10 (TreeStar) using fluorescence minus one (FMO) controls. Statistical analyses were performed on GraphPad Prism 7 using two-way ANOVA with Bonferroni post-hoc corrections.

Animal models

Animal protocols were in compliance with the regulations of Washington University School of Medicine Animal Studies Committee. Six- to 10-week-old NOD.Cg-*Prkdc*^{scid} *Il2rg*^{tm1Wjl}/SzJ (NSG) were used in all mice experiments. Both male and female mice were used in all experiments and randomly assigned to a treatment group.

CCRF-CEM xenograft model

The anti-leukemic effect of the CD7$^{\Delta}$CAR7 was tested in vivo using the T-ALL cell line, CCRF-CEM, modified to over express GFP and click-beetle red luciferase (CBR). NSG mice were injected into the tail vein with 5×10^5 CCRF-CEM$^{CBR\text{-}GFP}$ on day 0. Both male and female mice were used. CAR-T (2×10^6) were injected into the mice receiving CCRF-CEM$^{CBR\text{-}GFP}$ cells on day +4. To track CCRF-CEM$^{CBR\text{-}GFP}$ tumor growth in vivo, mice were injected intraperitoneally with 50 µg/g D-luciferin (Biosynth, Itasca, IL, USA) and imaged as previously described [21, 22]. Log-rank (Mantel-Cox) test was used to determine significant differences in survival. Statistical analysis of tumor burden, as defined by BLI imaging, was determined using two-way ANOVA for repeated measurement data, followed by a step-down Bonferroni adjustment for multiple comparisons. BLI was performed in blinded fashion.

Patient-derived xenograft model

T-ALL PDX DFCI12 was obtained from the Public Repository of Xenografts (PRoXe). http://www.PRoXe.org. NSG

were engrafted with 1×10^6 PDX DFCI12 cells on day 0 followed by infusion of 2×10^6 UCART7, UCART19, TRAC$^{\Delta}$, or WT T on day +1. Peripheral blood and spleens were analyzed by flow cytometry on week. Red blood cells were lysed using Red Blood Cell Lysing Buffer (Sigma-Aldrich) and washed with ice-cold PBS. Samples were prepared for flow cytometry by re-suspending cells in staining buffer (PBS supplemented with 0.5% bovine serum albumin and 2 mM EDTA) and incubating for 30 min at 4 °C with pre-titrated saturating dilutions of the following fluorochrome-labeled monoclonal antibodies; CD34-PE, CD7-BV421, CD4-APC, CD8-PECy7, mCD45-BV510, and hCD45-APC-H7. Full details of antibodies can be found in Supplemental Table 5. Antibodies were purchased from BD Biosciences unless otherwise stated. Data were analyzed using FlowJo V10.

Off-target analysis

Genomic insertion of dsODN

Blunt double-stranded oligodeoxynucleotide double-stranded oligonucleotide (dsODN) For_/5Phos/G*T*TTAATTGAGTTGTCATATGTTAATAACGGT*-A*T and Rev_5Phos/A*T*ACCGTTATTAACATATGA-CAACTCAATTAA*A*C and were prepared by annealing two modified oligonucleotides (Integrated DNA Technologies, IA) as previously described [23]. * represents phosphorothioate linkage and 5phos represents 5′ phosphorylation. CRISPR/Cas9 gene editing of primary T cells was performed as described previously, but with the addition of 100 pmol dsODN. Cells were cultured for an additional 7 days prior to harvest and DNA extraction (DNAeasy Qiagen GmbH, Germany).

dsODN capture

Hybrid capture of small discreet genomic loci can prove to be difficult without certain bait design and protocol modifications. Here, we enrich for fragments that contain a 34 bp DNA dsODN utilizing modified xGEN lockdown probes that are complimentary to the inserted dsODN sequence. The xGen lockdown probes have been designed to participate in a competitive hybridization manner to maximize hybrid pull-down efficiency. The novel design consists of multiple probes interrogating the tag region with a 2 base offset design. Additionally, the modified xGen Lockdown Probes were designed to enhance target sequence binding to the approximate melting temperature of standard 120 nt DNA xGen Lockdown probes. The streptavidin/biotin-mediated pull-down mechanism has also been modified to augment the result of an enriched subset of gDNA containing the 34 bp tag.

Automated dual indexed libraries were constructed with 250 ng of genomic DNA utilizing the KAPA HTP Library Kit (KAPA Biosystems) on the SciClone NGS instrument (Perkin Elmer) targeting 250 bp inserts (Supplemental Table 3). Libraries were enriched for eight PCR cycles. Sixteen libraries were pooled pre-capture generating a 5 µg library pool. The library pool was hybridized with a custom set of xGen Lockdown Probes (IDT), targeting the 34 bp ODN sequence. The concentration of the captured library pool was accurately determined through qPCR (KAPA Biosystems) to produce cluster counts appropriate for the Illumina HiSeq4000 platform. Total of 2×150 sequence data generated an average of 3.5 Gb of data per sample.

GUIDE-seq

The 16 existing dual indexed KAPA libraries constructed for the targeted capture experiment (Supplemental Table 3) were utilized for the Guide-Seq amplifications. PCR reactions were set up with 20 ng of existing library per sample, KAPA HiFi Hotstart Readymix (KAPA Biosystems), and 10 µM primers. PCR conditions can be found in Supplemental Table 4; GUIDE-seq indexed primers (GSiPs) were designed to target the sense and antisense Guide-seq ODN sequence while incorporating the P7 engraftment sequence and 8 bp sample index. Thirty-two amplicon libraries (16 sense and 16 antisense) were accurately quantitated through qPCR (KAPA Biosystems) to produce cluster counts appropriate for the Illumina HiSeq4000 platform. The amplicon libraries were normalized and pooled together. The amplicon library pool and targeted capture pool were combined in equal molar concentrations prior to generating one lane of HiSeq4000 2×150 sequence data (Illumina).

Sequencing data analysis

Sequence was aligned to the reference genome (build GRCh37-lite) using BWA MEM v0.7.10. A modified version of the guide-seq package [23] was used to identify 10-bp sliding windows, where the target sequence was present with at least 10 reads of support. To characterize off-target alignments, 35 bp of reference sequence flanking both sides of the breakpoint was retrieved and aligned with the observed sequence. Sites were required to have at least one supporting read in both the forward and reverse directions to be retained. Any site also identified in one of the control samples was removed.

Statistical analysis

The determination of sample size and data analysis for this study followed the general guideline for animal studies [24].

The distributions of time-to-death were described using Kaplan–Meier product limit method and compared by log-rank test. All the other in vivo data were summarized using means and standard deviations. The differences were compared using two-sample Student's *t*test, one-way ANOVA, or two-way ANOVA for repeated measurement data as appropriate, followed by ad-hoc multiple comparisons for between-group differences of interest (see also details for specific info of each Figure). Based on the law of diminishing returns, Mead recommended that a degree of freedom (DF) of 10–20 associated with error term in an ANOVA will be adequate for a pilot study to estimate preliminary information [25]. The normality of data was assessed graphically using residuals and the similarity of variance across groups was also assessed visually by checking the estimated variance of each group. A logarithm transformation was performed as necessary to better satisfy the normality and homoscedasticity assumptions. The resultant *p*values were adjusted by a step-down Bonferroni adjustment for multiple comparisons if needed. Comparing to the widely used Bonferroni adjustment, a step-down method is more powerful (smaller adjusted *p* values) while maintaining strong control of the familywise error rate. All analyses were two-sided and significance was set at a *p*value of 0.05. The statistical analyses were performed using SAS 9.4 (SAS Institutes, Cary, NC).

Results

CD7-CAR-T induce substantial fratricide

To generate the CD7-CAR-T (CART7), an anti-CD7 single chain variable fragment (scFv) was commercially synthesized and cloned into a third-generation CAR backbone with CD28 and 4-1BB internal signaling domains. The extracellular domain of hCD34 was added after a P2A peptide to enable both the detection of CAR following viral transduction and purification using anti-hCD34 magnetic beads (Fig. 1a) [26]. CAR-T targeting CD19 (CART19) were used as an irrelevant CAR-T control. Following transduction of T cells, there were significantly fewer CART7 than CART19 (Fig. 1b). In addition, CART7 were biased toward a CD4 phenotype when compared to CART19 (Supplemental Table 6).

Deletion of CD7 by CRISPR/Cas9

To prevent fratricide, we deleted CD7 in CAR-T using CRISPR/Cas9 gene editing. Ten guide RNAs (gRNA) targeting CD7 were designed and validated for activity (Supplemental Table 2). Plasmids encoding the gRNA and Cas9 were electroporated into the K562 leukemia cell line. CD7g4 and CD7g10 had the highest gene-editing efficiencies, as determined by targeted deep-sequencing across the CD7 locus (Fig. 1c) and were selected for further investigation. CD7g4 and CD7g10 guides were commercially synthesized, incorporating 2′-*O*-methyl and 3′phosphorothioate bases at the three terminal bases of the 5′ and 3′ of the gRNA to protect from nucleases activity [18]. We next tested the efficacy of gene editing by both CD7g4 and CD7g10 in human primary T cells. Activated T cells were electroporated with gRNA and Cas9 mRNA (Fig. 1d) and CD7 expression analyzed by flow cytometry on day +7. CD7g4 was the most effective at deleting CD7 expression, reducing the percentage of CD7+ T cells from 98.8 ± 0.17% to 9.1 ± 1.74% (Fig. 1e). Effective disruption of the CD7 locus was confirmed by targeted deep sequencing with indels observed in 89.14% of CD7 sequence reads (Fig. 1e). Only minimal loss of viability was observed 24 h post electroporation (Fig. 1e). As CD7g4 was most effective at deleting expression of CD7 in T cells, all future experiments were performed using CD7g4.

CD7$^{\Delta}$CART7 prevents fratricide and kills T-ALL in vitro and in vivo

Next, we generated CART cells deficient in expression of CD7. We performed CRISPR/Cas9 gene editing of CD7 in primary T cells followed by transduction of CD7-edited T cells (CD7$^{\Delta}$) with CAR7 (Fig. 2a) to generate CD7$^{\Delta}$CART7. We anticipated that there would be a low level of fratricide resulting from residual CD7 surface expression following gene editing, and this was confirmed by a moderate reduction in CD7$^{\Delta}$CART7 yield relative to CD7$^{\Delta}$CART19 (7.5-fold vs. 12.6-fold expansion over 6 days Fig. 2a). Autologous T cells transduced with GFP were effectively killed by CD7$^{\Delta}$CART7 but not by CD7$^{\Delta}$CART19 confirming the requirement for CD7 deletion in CART targeting CD7 (Fig. 2b). Finally, in contrast to CD7$^{\Delta}$CART19, CD7$^{\Delta}$CART7 effectively killed CD7+ T-ALL cell lines MOLT-4 (70% CD7+), MOLT-3 (96% CD7+) and HSB-2 (99% CD7+) as determined by 4 h Cr release assays (Fig. 2c).

To assess the activity of CD7$^{\Delta}$CART7 in a xenogeneic model of T-ALL, 5×10^5 Click Beetle Red luciferase (CBR) labeled CCRF-CEM T-ALL (99% CD7+ by FACS) cells were injected I.V. into NSG recipients prior to infusion of 2×10^6 CD7$^{\Delta}$CART7 or non-targeting CD7$^{\Delta}$CART19 control cells on day +4 (Fig. 3a). In contrast to mice receiving CD7$^{\Delta}$CART19, or mice injected with tumor only, mice receiving CD7$^{\Delta}$CART7 had significantly prolonged survival ($p = 0.0003$, Fig. 3b) and reduced tumor burden as determined by bioluminescent imaging (BLI) (Fig. 3c). CD7$^{\Delta}$CART7-treated mice exhibited signs of GvHD and,

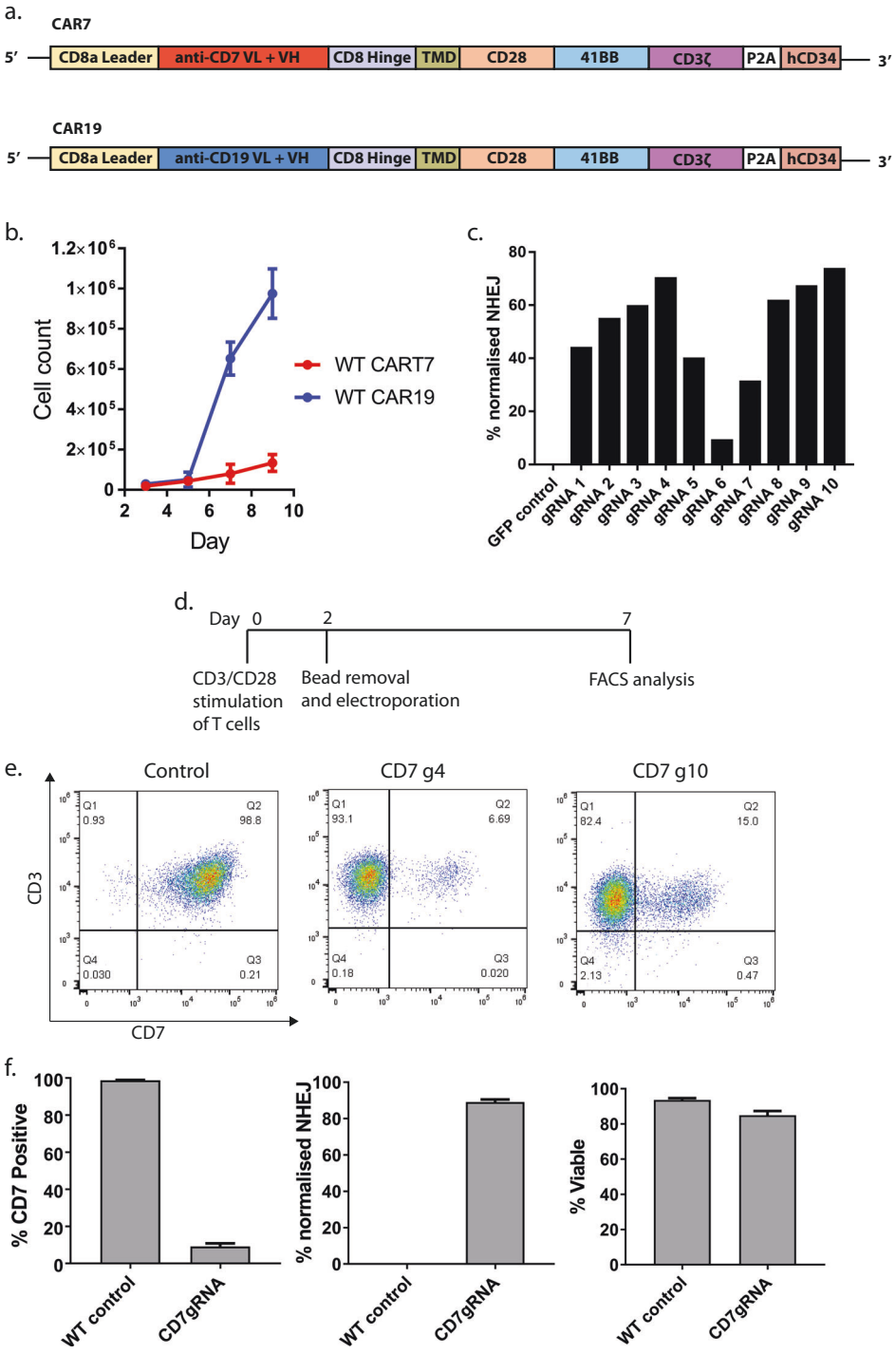

Fig. 1 CART7 induce fratricide. **a** Schematic of CAR constructs. **b** T cells were cultured in Xcyte media supplemented with 50 U/mL IL-2 and 10 ng/ml IL-15 in the presence of anti-CD3/CD28 beads (bead to cell ratio, 3:1). On day 3, the beads were removed, and 2.5×10^4 cells were plated in each well of a 96-well plate prior to transduction with either CAR7 or CAR19. CART7 undergo fratricide and fail to demonstrate robust expansion in the days following transduction (Day 9 CART7 = 13.7% of CART19 cell count $n = 3$ mean ± s.d). **c** Editing efficiencies of gRNA targeting CD7. % NHEJ determined as a percentage of sequencing reads with indels relative to WT cells. **d** Schema of CRISPR/Cas9 gene editing of human T cells. **e** CD7 gRNA editing efficiencies in human primary T cells as determined by FACS. **f** Percentage of CD7+ T cells following gene editing with CD7g4. ($n = 3$ mean ± s.d.). **i** Targeted deep sequencing of CD7 locus following CRISPR/Cas9 gene editing with CD7g4 ($n = 3$ mean ± s.d.). Viability of primary T cells following CRISPR/Cas9 gene editing with CD7g4, determined 24 h post electroporation ($n = 3$ mean ± s.d.)

consistent with previous reports [27–29], most mice eventually succumbed to leukemia. To assess efficacy of CD7$^{\Delta}$CART7 against patient primary T-ALL cells, CAR-T were tested against patient-derived xenografts. However, T-ALL blasts were only detectable in mice receiving tumor only and were eliminated in mice receiving either CD7$^{\Delta}$CART7 or CD7$^{\Delta}$CART19 suggesting that CD7$^{\Delta}$CART7 and CD7$^{\Delta}$CART19 maintain alloreactivity in vivo in NSG mice (Supplemental Fig. 1).

Double deletion of TRAC and CD7 in CART7 prevents fratricide and GvHD, and maintains robust CD7-directed T-ALL killing

To overcome alloreactive barriers that limit the use of non-self T cells, due to the risk of lethal GvHD, we generated CAR-T in which both CD7 and the TRAC were genetically deleted. The gRNA sequence, targeting TRAC, was obtained from Osborn et al. [30]. T cells were activated

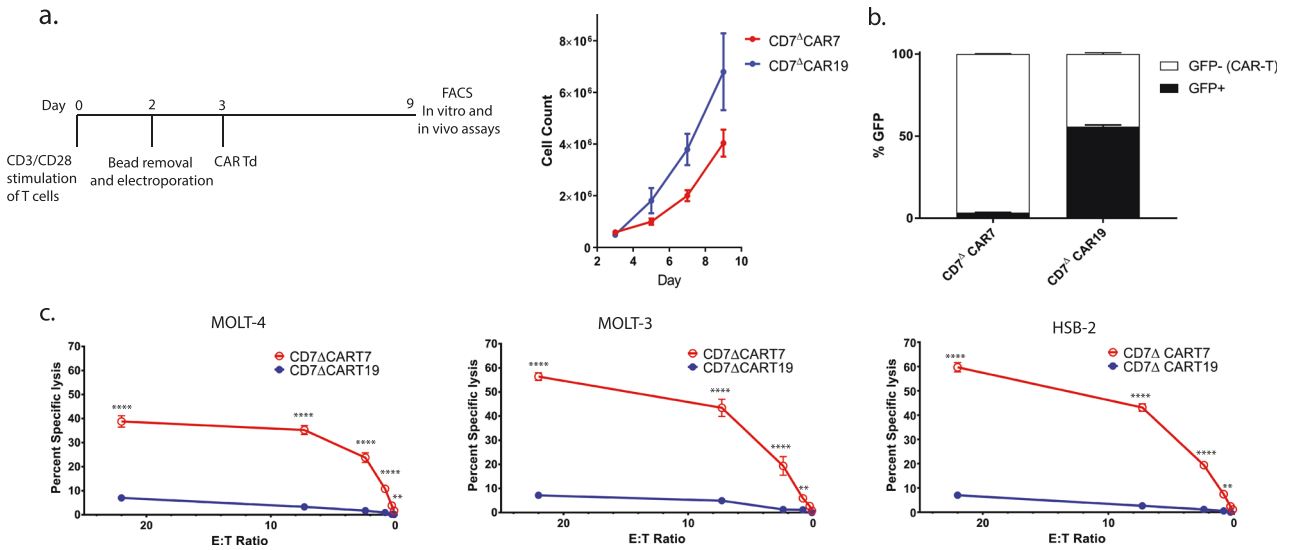

Fig. 2 CD7$^{\Delta}$CART7 effectively kills T-ALL cell lines in vitro and in vivo. **a** Schema of gene-edited CAR-T generation. Cell counts as determined using a Nexcelom Cellometer with ViaStain^{TM} ($n = 3$ mean ± s.d). **b** WT T cells transduced with lenti-GFP (GFP+ T cells) were used as targets and were co-incubated with CD7$^{\Delta}$CART7 or CD7$^{\Delta}$CART19 at a ratio of 1:1 for 24 h. The percentage of GFP+ T cells in the population was determined by flow cytometry. **c** In vitro killing assay. CD7$^{\Delta}$CART7 or CD7$^{\Delta}$CART19 were cultured with [51Cr]-labeled MOLT-3, MOLT-4, or HSB-2 at various E:T ratios for 4 h

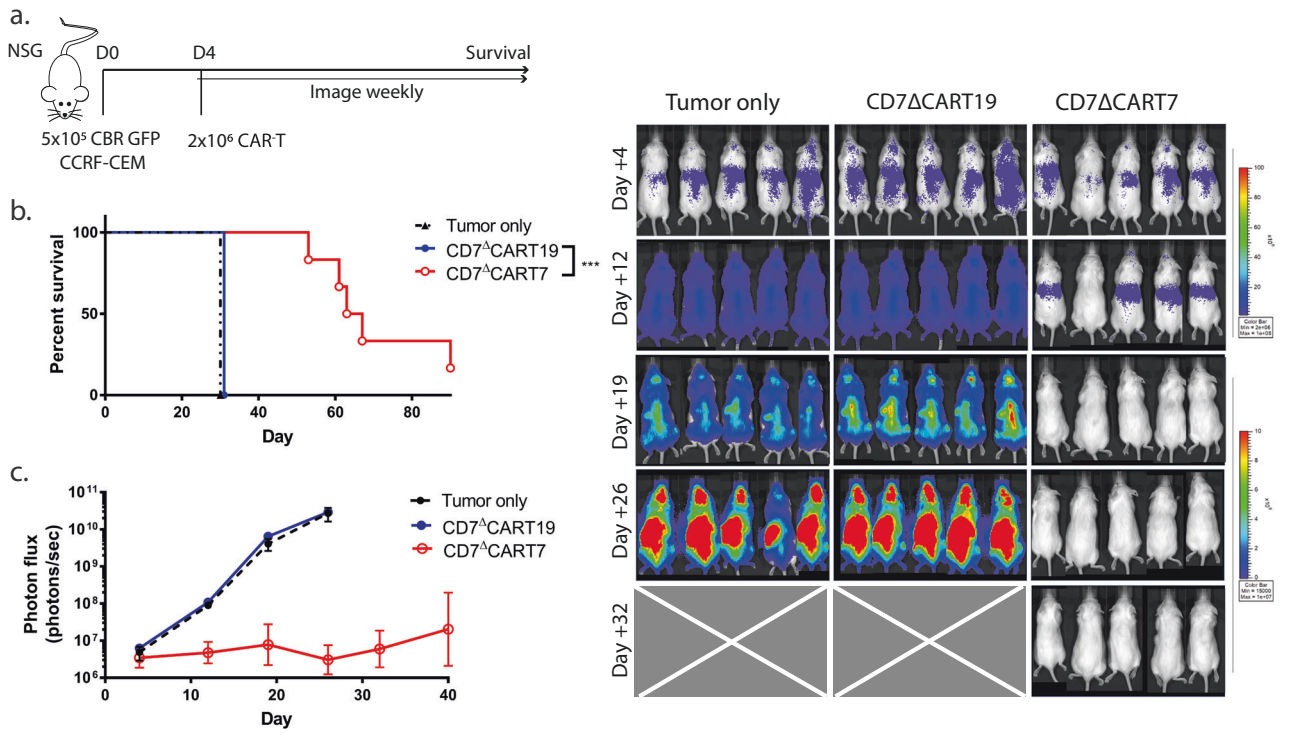

Fig. 3 In vivo efficacy of CD7$^{\Delta}$CART7. **a** Schema of xenogeneic mouse model of T-ALL. NSG mice were injected with 5×10^5 CCRF-CEM$^{CBR\text{-}GFP}$ cells on day 0, then infused with 2×10^6 CD7$^{\Delta}$CART7 or CD7$^{\Delta}$CART19 on day +4. **b** Kaplan–Meier survival curve of mice treated with CD7$^{\Delta}$CART7 or CD7$^{\Delta}$CART19. Median survival CD7$^{\Delta}$CART19-treated mice, 31 days vs. CD7$^{\Delta}$CART7-treated mice, 65 days; $p = 0.0003$) and **c** tumor burden as determined by BLI imaging. p values <0.05 considered significant, $^{*}p \le 0.05$, $^{**}p \le 0.01$, $^{***}p \le 0.001$, $^{****}p \le 0.0001$

using anti-CD3/CD28 beads for 2 days prior to bead removal and electroporation with 20 µg of CD7g4, 20 µg of TRACg, and 15 µg of spCas9 mRNA (Fig. 4a). Multiplex CRISPR/Cas9 gene editing resulted in the simultaneous deletion of CD7 and TRAC in 72.8 ± 1.92% of cells, as determined by FACS analysis (Fig. 4a).

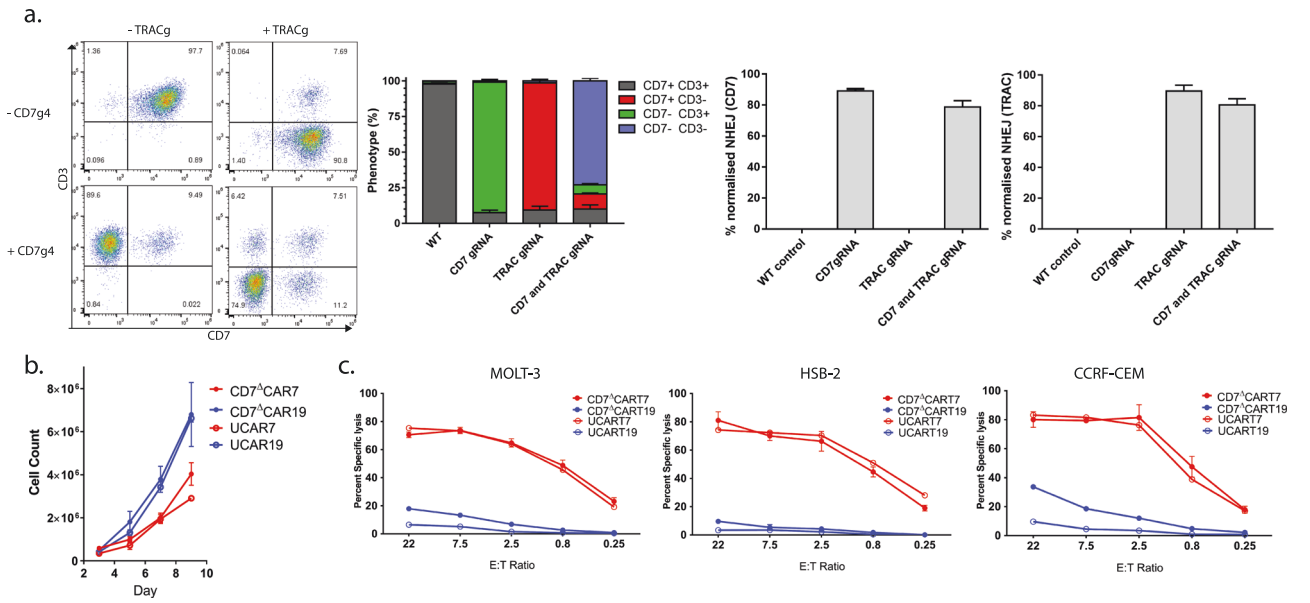

Fig. 4 UCART7, deficient in CD7 and TRAC, effectively kill T-ALL cell lines in vitro. **a** Multiplex gene editing results in high efficiency double deletion of TRAC and CD7 as determined by FACS and targeted deep sequencing of the CD7 and TRAC loci. **b** CD7$^{\Delta}$CART7 and UCART7 exhibit robust expansion, but yield fewer cells likely due to fratricide of both the residual non-gene-edited T cells and persistent CD7 surface expression on gene-edited cells (which lags genetic deletion). **c** CD7$^{\Delta}$CART7, UCART7, and their respective CD19 control CAR-T cells were cultured with [51Cr]-labeled MOLT-3, HSB-2, or CCRF-CEM cells at various E:T ratios for 4 h. UCART7 was equal to CD7$^{\Delta}$CART7 in efficiency of killing the CD7+ T-ALL cell line in vitro, even at low effector to target ratios. Statistical significance was determined using one-way ANOVA, followed by a step-down Bonferroni adjustment for multiple comparisons ($n = 3$ mean ± s.d). p values <0.05 considered significant, $^{*}p \le 0.05$, $^{**}p \le 0.01$, $^{***}p \le 0.001$, $^{****}p \le 0.0001$

In keeping with recent nomenclature in the field, our CD7$^{\Delta}$TRAC$^{\Delta}$CART7 was termed universal CART7 or UCART7 [31]. UCART7 was as effective as CD7$^{\Delta}$CART7 at killing T-ALL cell lines in vitro. UCART7 had no proliferation defect when compared to CD7$^{\Delta}$CART7, however, as observed with CD7$^{\Delta}$CART7, UCART7 resulted in moderately reduced CAR-T proliferation and yield relative to the CD19 control CART (Fig. 4b). Since incomplete gene editing of TRAC leaves residual potentially alloreactive CD3^{+} CAR-T, these were depleted by negative selection using anti-CD3 magnetic beads on day +8. Both UCART7 and CD7$^{\Delta}$CART7 killed CD7+ T-ALL cell lines, MOLT3, CCRF-CEM, and HSB-2 in vitro with equally high efficiencies demonstrating no loss of efficacy upon double deletion of CD7 and TRAC (Fig. 4c). Interestingly, non-specific killing by UCART19 was attenuated at high effector to target (E:T) ratios when compared to CD7$^{\Delta}$CART19, suggesting loss of alloreactivity following TRAC deletion.

We next tested the ability of UCART7 to kill primary T-ALL blasts in vitro. Due to the similarity of antigen expression between primary T-ALL and CAR-T, total leukocytes containing T-ALL from patients (83.9–99.6% CD7 + cells) were labeled with CFSE to clearly distinguish T-ALL from CAR-T. Patient cells were incubated with CAR-T at a ratio of 1:1 for 24 h. Both CD7$^{\Delta}$CART7 and UCART7 killed an average of 95% of cells across all three primary samples, relative to the respective CD19 control CAR-T (Fig. 5a), thus demonstrating efficacy against human primary T-ALL in vitro.

In light of the anti-tumor activity, we observed when either CD7$^{\Delta}$CART and CD7$^{\Delta}$CART19 were infused into primary T-ALL PDX bearing NSG mice (Supplemental Fig. 1), we tested the capacity of UCART7 to kill primary T-ALL in vivo without inducing an alloreactive Graft-vs.-Leukemia effect (GvL) or xenogeneic GvHD (Fig. 6). Recipients of T cells edited to delete TRAC (TRAC$^{\Delta}$) exhibited high tumor burden in both the blood and spleen (Fig. 6b) when compared to recipients of WT T cells (day +48 spleen $p < 0.0001$, blood $p = 0.0001$), demonstrating an inability of TRAC$^{\Delta}$ to induce allogeneic GvL. Furthermore, considerable expansion of alloreactive T cells (Fig. 6a) and severe GvHD (mean clinical GvHD score = 5.66, Fig. 6c) was observed in recipients of WT T cells. In contrast, GvHD was completely absent and T cells undetectable in mice receiving TRAC$^{\Delta}$ T cells (Fig. 6c). T-ALL blasts were absent in peripheral blood of mice receiving UCART7 in comparison to mice receiving UCART19 with T-ALL comprising >56% of total CD45^{+} cells in these mice ($p < 0.0001$), similar to the high tumor burden observed in PDX only controls (Fig. 6b). Concordant results were observed in the spleen (Fig. 6b, UCART7 < 3% T-ALL vs. UCART19 = 85.87% T-ALL; $p < 0.0001$), with TRAC$^{\Delta}$ T cells, UCAR19 and PDX only recipient mice exhibiting

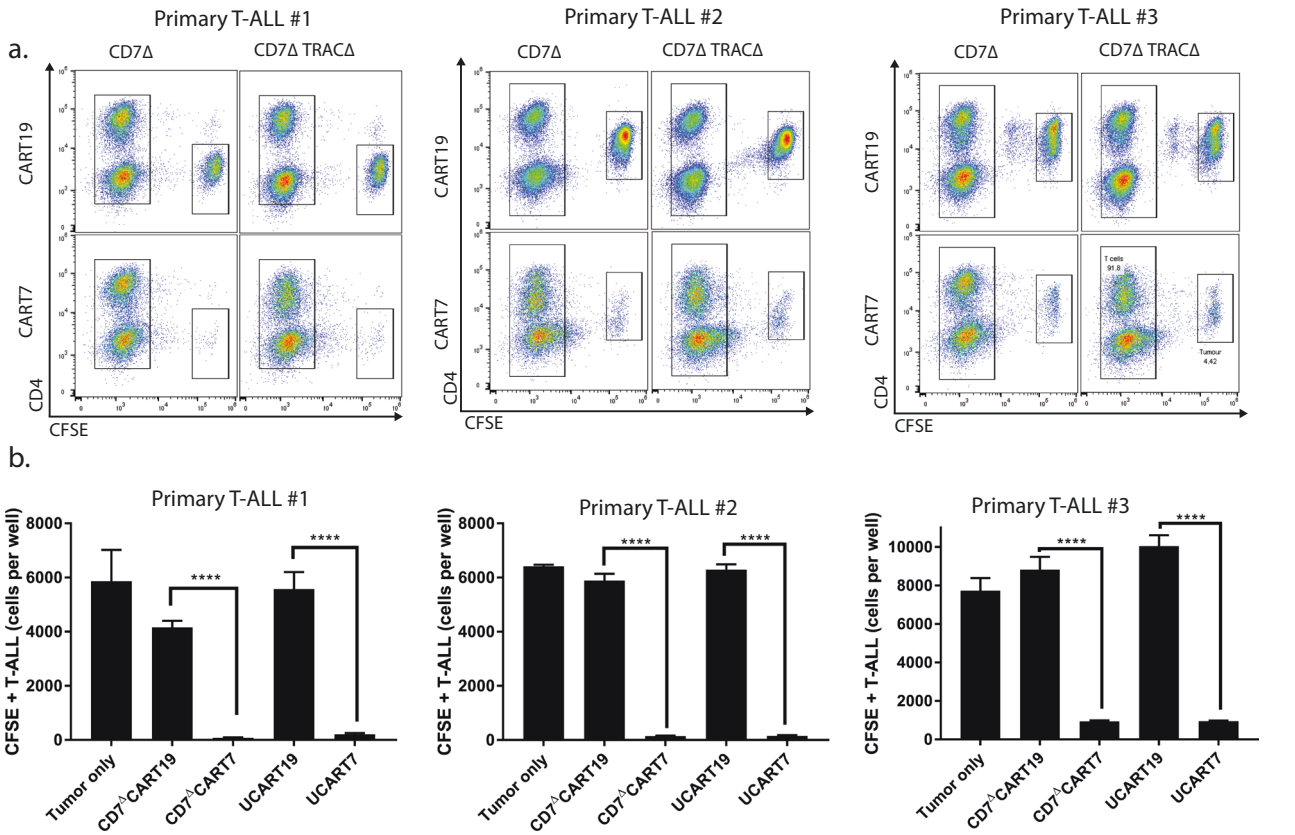

Fig. 5 UCART7 kills primary patient T-ALL blast in vitro. Primary blasts obtained from three individual patients with CD7+ T-ALL were labeled with 150 nM CFSE. Labeled cells were co-incubated at a 1:1 ratio with either CD7$^{\Delta}$CART7, UCART7, or their respective CD19 controls in triplicate for 24 h prior to FACS analysis. Accucount florescent beads were used to determine actual cell counts. Data were collected using a Gallios cytometer. **a** Representative FACS plots. **b** CD7$^{\Delta}$CAR7 and UCART7 effectively killed T-ALL blasts relative to CD7$^{\Delta}$CAR19 and UCART19 ($n = 4$). Data were compared using one-way ANOVA, followed by ad-hoc multiple comparisons for between-group differences, and a logarithm transformation was also performed. p values <0.05 considered significant, *$p \le 0.05$, **$p \le 0.01$, ***$p \le 0.001$, ****$p \le 0.0001$

splenomegaly. In stark contrast, UCART7 recipients had normal-sized spleens (data not shown). Furthermore, unlike UCART19, UCART7 were detectable 6 weeks' post injection as detected by the hCD34 epitope, demonstrating persistence of UCART7 in vivo (Supplemental Fig. 2).

Off-target nuclease activity

High efficiency gene editing with CRISPR/Cas9 can induce undesirable off-target genetic changes that could have potentially detrimental effects on the biology of these T cells and subsequently on the recipients that receive UCART7 infusions. We used two different techniques to assess off-target genetic changes in human primary T cells, both of which rely on the insertion of a small double-stranded oligodeoxynucleotide (dsODN) at DNA double-strand breaks. The first protocol utilized a modified version of GUIDE-seq [23], without the inclusion of barcoded indexes, to specifically amplify target sites surrounding the inserted dsODN using PCR; the second technique used integrated DNA technologies (IDT) to capture probes to enrich loci containing the target dsODN sequence. Both techniques use next-generation sequencing to identify the loci of inserted dsODN. To ensure identification of bona fide sites of off-target nuclease activity, each condition (CD7g4, TRACg, and combined CD7g + TRACg) was performed in triplicate, generating an average 1.26×10^6 sequencing reads per replicate. Loci with bidirectional sequencing reads >10× coverage were included in the analysis. First, we assessed the ability of each technique to identify on-target sites. Both GUIDE-seq and dsODN capture robustly identified sites of on-target activity, with each on-target site generating between 300× and 22,000× coverage across all three replicates in each condition (Table 1). Next, we assessed off-target nuclease activity using the same stringency. GUIDE-seq revealed a single off-target site in multiplex edited T cells (CD7g4 + TRACg), an intronic insertion in RBM33, present in all three replicates. No off-target sites were observed when assessed by dsODN capture despite high coverage of on-target activity (Table 1). Upon relaxing, the stringency of GUIDE-seq analysis to include potential off-target sites present in two

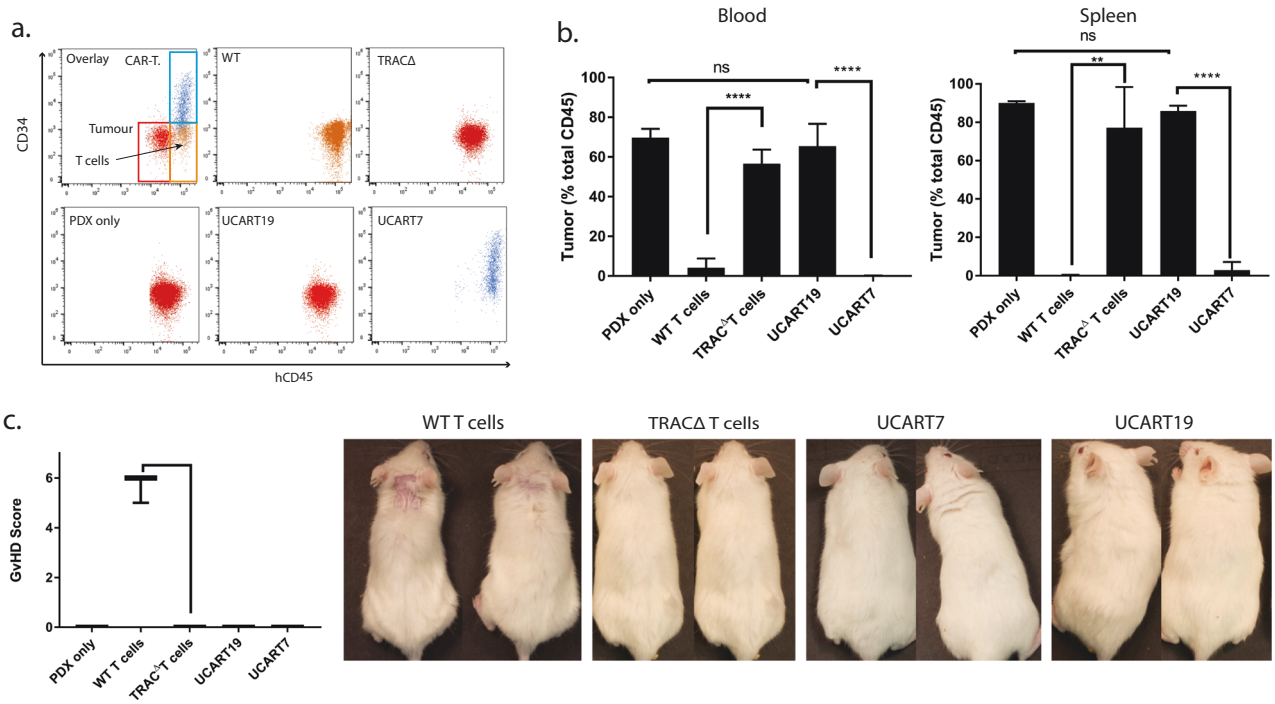

Fig. 6 UCART7 kills primary patient T-ALL blast in vivo without inducing xenogeneic GvHD. NSG were engrafted with 1×10^6 PDX DFCI12 cells on day 0 followed by infusion of 2×10^6 UCART7, UCART19, TRAC$^{\Delta}$, or WT T on day +1. Mice were assessed for GvHD, and blood and splenocytes analyzed by FACS 6 weeks post CAR-T injection. **a** Representative flow cytometry plots of blood analysis presented to show both tumor and T cells. **b** Percentage of tumor cells out of total mouse and human CD45 cells in the blood (WT $n = 6$, UCART7 $n = 6$, UCART19 $n = 6$, TRAC$^{\Delta}$ $n = 4$ or PDX only $n = 5$) and spleens ($n = 3$). Unlike TRAC$^{\Delta}$ T cells, WT T cells clear tumor through an alloreactive GvL effect (blood, $p < 0.0001$; spleen, $p = 0.0033$). UCART7 is effective at clearing PDX relative to UCART19 (blood, $p < 0.0001$; spleen $p < 0.0001$). **c** Clinical GvHD scores, graded according to Cooke et al. [42] ($n = 3$ mean ± s.d.). Unlike TRAC$^{\Delta}$ T cells, WT T cells induce GvHD. Representative images of mice following infusion of WT T cells, TRAC$^{\Delta}$ T cells, UCART7, and UCART19. *$p \le 0.05$, **$p \le 0.01$, ***$p \le 0.001$, ****$p \le 0.0001$

or more replicates, we identified four additional potential off-target sites for CD7g and four sites for TRACg. One additional sit of potential off-target activity for multiplexed CD7 and TRAC gene editing was identified (Table 1). Loci identified by GUIDE-seq were not present in the data obtained using dsODN capture, nor were additional sites of off-target nuclease activity identified following analysis of these data with reduced stringency. In addition, dsODN capture allows the identification of gene rearrangements between multiple sites of on-target nuclease activity, however, no gene rearrangements were observed between CD7 and TRAC following multiplex gene editing. These results suggest that high-efficiency CRISPR/Cas9 gene editing of primary T cells with CD7g4 and TRACg, individually or in combination, is not associated with significant off-target activity or on-target gene rearrangements, using these platforms.

Discussion

In this report, we demonstrate the generation of CRISPR/Cas9 genetically edited human T cells lacking both CD7 and TRAC. Lentiviral transduction of these genetically edited T cells with a CD7-CAR (UCART7) allows for efficient killing of CD7+ primary human T-ALL and T-ALL cell lines in vitro and in vivo without consequent fratricide or T cell-mediated xenogeneic GvHD. This represents an "off-the-shelf" strategy for targeted treatment of T cell neoplasms that merits further clinical investigation. This work improves upon previous CAR-T targeting T cell malignancies, which induce partial fratricide and overlook barriers for the collection and separation of adequate normal T cells from malignant cells. Pinz et al. described the preclinical development of a CD4-targeted CAR-T, which maintained CD8+ CAR-T-mediated cytotoxicity of CD4+ targets resulting in complete CD4+ T cell loss [32]. Likewise, Mamonkin et al. described a CD5-targeted CAR-T that induces only transient fratricide, allowing sufficient CD5 CAR-T expansion despite almost universal expression of CD5 on activated WT T cells [29].

We chose to target CD7 due to high expression in the majority of T-NHL and T-ALL [10–12]. In addition to T cell malignancies, CD7 is expressed in ~24% of AML and is thought to be marker of leukemic stem cells [33, 34] and expressed in the vast majority of both natural killer (NK)

Table 1 Sites of nuclease activity identified using GUIDE-seq and DsODN capture

GUIDE seq		CD7g4		TRACg		CD7g + TRACg		
Position	Gene	Total reads (mean)	# of replicates	Total reads (mean)	# of replicates	Total reads (mean)	# of replicates	
Chr17:80274575	**CD7**	**501**	**3**	**-**	**-**	**326**	**3**	**On-target**
Chr14:23016519	**TRAC**	**-**	**-**	**2843**	**3**	**1171**	**3**	**On-target**
Chr7:155492215	RBM33 (Intron)	-	-	-	-	739	3	Off-target
Chr18:57136752	CCBE1 (Exon)	15	2	-	-	-	-	Off-target
Chr5:124638037	Intergenic	78	2	-	-	-	-	Off-target
Chr2:131741952	ARHGEF4 (Intron)	188.5	2	-	-	-	-	Off-target
Chr6:163217520	PACRG	292	2	-	-	-	-	Off-target
Chr4:49659204	Intergenic	-	-	278	2	-	-	Off-target
Chr5:100549449	Intergenic	-	-	127	2	-	-	Off-target
Chr4:102319592	Intergenic	-	-	112.5	2	-	-	Off-target
Chr5:163357022	Intergenic	-	-	53.5	2	-	-	Off-target
Chr2:177340112	Intergenic	-	-	-	-	51.5	2	Off-target
DsODN Capture								
Chr17:80274575	**CD7**	**2268**	**3**	**-**	**-**	**2163**	**3**	**On-target**
Chr14:23016519	**TRAC**	**-**	**-**	**22,632**	**3**	**22,810**	**3**	**On-target**

On-target activity is highlighted in bold. For technical details of analysis, please refer to the "Methods"

and NKT NHLs and leukemias. Thus, CART7 could be used to treat myeloid as well as both T and NK lymphoid malignancies. Furthermore, we wanted to target an antigen which could be deleted in T cells without impacting immune function. Mice with genetic deletion of CD7 are phenotypically normal, with normal lymphocyte populations and maintain T cell activity in response to allogeneic and mitogenic stimuli [35]. Thus, CD7 is a candidate for gene editing of CAR-T to target both AML and T cell malignancies.

In our study, there was extensive fratricide when CART7 was used without CD7 deletion with surviving CART7 predominantly CD4+ and CD7− [36]. These data underline the importance of using CART7, which are themselves devoid of CD7. Such cells provide optimal resistance to fratricide while allowing expansion of cytotoxic CD8 T cells with balanced expansion of CD4 cells. Indeed, high efficiency CRISPR/Cas9-mediated CD7 genetic deletion mitigated CAR7 fratricide, and upon CD7 protein loss (which may lag genetic deletion), the cells demonstrated complete fratricide resistance.

The use of autologous T cells for the generation of CART7 presents unique challenges. First, patients with relapsed T-ALL and T-NHL are often heavily pretreated with T cell poisons such as purine nucleoside analogs (fludarabine, cladribine, and nelarabine) and T cell cytotoxic monoclonal antibodies (Campath) [37, 38]. Therefore, the number and function of T cells may be markedly reduced limiting the efficient generation, sufficient numbers, and function of CART7 for therapeutic benefit. Second, most T cell hematologic malignancies and normal T effectors co-express many of the same surface antigens making it very difficult to purify normal T effectors from the malignant T cells for genetic editing and lentiviral transduction. If the process of T cell purification is not absolute there will be a risk of deleting CD7 within the malignant T cell population. Deletion of the target gene in contaminating malignant T cells would result in a clone resistant to CD7$^{\Delta}$CART7 therapy. Thus, the potential contamination risk of normal effector T cells with malignant T cell precludes the use of patient-derived T cells to generate CAR-T cells for T cell malignancies. These challenges have not been addressed in previous manuscripts describing CAR-T-targeting T cell malignancies in which the target antigen is genetically deleted, or target expression suppressed within the CAR-T [27, 28]. Consequently, we have further modified our CD7$^{\Delta}$CART7 by editing out TRAC permitting the use of allogeneic donor T cells without the risk of inducing GvHD. Following the success of the first-in human trial of UCART19, a TRAC edited non-alloreactive CAR-T to CD19 generated from allogeneic donor T cells [31], we developed UCART7 in which we have successfully deleted, with high efficiency and with minimal off-

target effects, both CD7 and TRAC by multiplex CRISPR/Cas9 gene editing. UCART7 killed T-ALL cell lines and primary patient T-ALL in vitro as effectively as CD7$^{\Delta}$CART7. Unlike CD7$^{\Delta}$CART7, which demonstrated alloreactive anti-leukemia activity against T-ALL PDX in vivo, UCART7 demonstrated robust CAR7-mediated killing independent of alloreactivity and without inducing GvHD. This suggests TRAC deletion does not alter CAR-mediated cytotoxicity while completely preventing GvHD. A similar strategy was recently employed by Qasim et al. for the delivery of UCART19 for the treatment of two pediatric patients with relapsed B cell acute lymphoblastic leukemia [31]. Qasim et al. deleted TRAC using TALEN-mediated gene editing in UCART19, demonstrating a complete response and persistence of this off-the-shelf allogeneic UCART19 in these two patients until bone marrow transplantation 3 months following CAR-T infusion. We acknowledge that Qasim et al. also deleted CD52 in UCART19 allowing for the administration of campath as conditioning to these patients, thus inhibiting recipient T and NK cells while having no such immunosuppressive effects on donor UCART19. Unlike UCART19, UCART7 would have the additional advantage of directly killing recipient alloreactive recipient T cells and NK cells (both CD7+ and targets for UCART7), thus potentially reducing or completely blocking the rejection of donor UCART7 by host T and NK cells. We have demonstrated that UCART7 is effective at killing CD7+ T cells in vitro, thus, rejection of UCART7 by host T cells is unlikely to be of significant concern. Indeed, some delayed rejection of CAR-T may by desirable in the long term as UCART7 persistence would maintain the recipient in an immunodeficient state due to reduced T cells and NK cells. Should rejection occur, UCART7 would still provide a viable bridge to transplantation, which many feel is the primary benefit of CAR-T, including CART19. Our expectation is that UCART7 will significantly prolong survival in patients with T cell hematological malignancies and provide a viable bridge to transplant. Despite observing UCART7 persistence in our immune-deficient PDX T models, clinical studies will be required to fully characterize UCART7 persistence and Host-vs-Graft effect in humans treated for T cell neoplasms. While we do not anticipate barriers to the development of human therapeutic UCART7, studies are currently underway to assess the viability of scaling UCART7 for clinical trials.

Although we did not observe robust off-target nuclease activity following CD7, TRAC, or multiplex gene editing, the recent development of high-fidelity Cas9 (SpCAS9-HF1) may further reduce the risk of undesirable genetic events [39]. Furthermore, insertion of the CAR directly into the TRAC locus, as recently reported [40, 41], or, potentially, the CD7 locus, would further mitigate the risk of oncogenic transformation from random viral vector integration into undesirable loci. Furthermore, our vector allows the inclusion of suicide genes such as thymidine kinase (TK), which we have previously shown in a first-in-man study to allow both the effective tracking of genetically modified T cells using [^{18}F]FHBG PET-CT imaging and the elimination of T cells in vivo [26]. This strategy would safeguard against potential toxicity or oncogenic transformation resulting from CRISPR/Cas9 gene editing and viral integration and allow the termination of therapy to prevent long-term T cell aplasia.

This study presents the first clinically feasible adoptive T cell gene therapy for T cell malignancies. Specifically, we show that CD7xTRAC multiplex gene editing of human T cells followed by lentiviral transduction with a third-generation CD7-CAR results in UCART7 that are resistant to fratricide and exhibit no alloreactivity or GvHD potential in vivo. This will allow for the use of "off-the-shelf" tumor-free allogeneic T cells as a source of CAR-T. The use of these genetically modified T cells in NSG mice carrying human T-ALL cell lines or primary human T-ALL tumors results in rapid and effective elimination of these tumors in vivo with no signs of xenogeneic GvHD. These findings warrant further efforts to translate these observations into the clinic specifically for the treatment of children and adults with relapsed and refractory T cell hematologic malignancies.

Data availability

The modified guide-seq code is available at https://github.com/chrisamiller/guideseq.

Acknowledgements This work is dedicated in memory of Gordon S. Cooper. 1946–2017. We thank Dr. Carl June (University of Pennsylvania) for providing the backbone of a third-generation CAR and the pELNS-Ef1α lentiviral vector.

Funding Specialized Program of Research Excellence (SPORE) in Leukemia NIH: 1P50CA171063-01A1, R35 CA210084-01A, the Gabrielle's Angels Foundation, the Children's Discovery Institute of Washington University and St. Louis Children's Hospital, the Alvin J. Siteman Cancer Research Fund at Washington University in St. Louis, MO.

Author contributions MLC and JFD conceived project. MLC, JFD, JC, and MR designed the experiments. MLC, JKR, JMN, and KE cloned the CAR constructs and generated virus. MLC performed gene editing and generated CAR-T. MLC, JKR, and JO preformed and analyzed in vitro assays. MLC, JKR, JMN, BW, and LNG performed in vivo experiments. JLP and SA performed BLI imaging. KS and MLC performed FACS analysis. DMW and AG developed PDX models. MLC, CAM, CCF, and RSF completed and analyzed off-target nuclease activity analysis. FG performed all statistical analyses. All authors were involved in the interpretation of data and preparation of this manuscript.

Compliance with ethical standards

Conflict of interest The authors declare that they have no conflict of interest.

References

1. Ma H, Abdul-Hay M. T-cell lymphomas, a challenging disease: types, treatments, and future. Int J Clin Oncol. 2017;22:18–51.
2. Karrman K, Johansson B. Pediatric T-cell acute lymphoblastic leukemia. Genes Chromosomes Cancer. 2017;56:89–116.
3. Gökbuget N, Arnold R, Böhme A, Fietkau R, Freund M, Ganser A. et al. Treatment of adult ALL according to protocols of the German Multicenter Study Group for adult ALL (GMALL). Editors: Estey EH, Faderl SH, Kantarjian HM. Acute leukemias. Berlin, Heidelberg: Springer Berlin Heidelberg; 2008. p. 167–76.
4. Marks DI, Paietta EM, Moorman AV, Richards SM, Buck G, DeWald G, et al. T-cell acute lymphoblastic leukemia in adults: clinical features, immunophenotype, cytogenetics, and outcome from the large randomized prospective trial (UKALL XII/ECOG 2993). Blood. 2009;114:5136–45.
5. Goldberg JM, Silverman LB, Levy DE, Dalton VK, Gelber RD, Lehmann L, et al. Childhood T-cell acute lymphoblastic leukemia: the Dana-Farber Cancer Institute acute lymphoblastic leukemia consortium experience. J Clin Oncol. 2003;21:3616–22.
6. Litzow MR, Ferrando AA. How I treat T-cell acute lymphoblastic leukemia in adults. Blood. 2015;126:833–41.
7. Porter DL, Hwang W-T, Frey NV, Lacey SF, Shaw PA, Loren AW, et al. Chimeric antigen receptor T cells persist and induce sustained remissions in relapsed refractory chronic lymphocytic leukemia. Sci Transl Med. 2015;7:303ra139–303ra139.
8. Kochenderfer JN, Dudley ME, Kassim SH, Somerville RPT, Carpenter RO, Stetler-Stevenson M, et al. Chemotherapy-refractory diffuse large B-cell lymphoma and indolent B-cell malignancies can be effectively treated with autologous T cells expressing an anti-CD19 chimeric antigen receptor. J Clin Oncol. 2015;33:540–9.
9. Park JH, Geyer MB, Brentjens RJ. CD19-targeted CAR T-cell therapeutics for hematologic malignancies: interpreting clinical outcomes to date. Blood. 2016;127:3312–20.
10. Campana D, Behm FG. Immunophenotyping of leukemia. J Immunol Methods. 2000;243:59–75.
11. Khalidi HS, Chang KL, Medeiros LJ, Brynes RK, Slovak ML, Murata-Collins JL, et al. Acute lymphoblastic leukemia. Survey of immunophenotype, French-American-British classification, frequency of myeloid antigen expression, and karyotypic abnormalities in 210 pediatric and adult cases. Am J Clin Pathol. 1999;111:467–76.
12. Patel JL, Smith LM, Anderson J, Abromowitch M, Campana D, Jacobsen J, et al. The immunophenotype of T-lymphoblastic lymphoma in children and adolescents: a Children's Oncology Group report. Br J Haematol. 2012;159:454–61.
13. Milush JM, Long BR, Snyder-Cappione JE, Cappione AJ 3rd, York VA, Ndhlovu LC, et al. Functionally distinct subsets of human NK cells and monocyte/DC-like cells identified by coexpression of CD56, CD7, and CD4. Blood. 2009;114:4823–31.
14. Carpenito C, Milone MC, Hassan R, Simonet JC, Lakhal M, Suhoski MM, et al. Control of large, established tumor xenografts with genetically retargeted human T cells containing CD28 and CD137 domains. Proc Natl Acad Sci USA. 2009;106:3360–5.
15. Roguska MA, Pedersen JT, Keddy CA, Henry AH, Searle SJ, Lambert JM, et al. Humanization of murine monoclonal antibodies through variable domain resurfacing. Proc Natl Acad Sci USA. 1994;91:969–73.
16. Dull T, Zufferey R, Kelly M, Mandel RJ, Nguyen M, Trono D, et al. A third-generation lentivirus vector with a conditional packaging system. J Virol. 1998;72:8463–71.
17. Zufferey R, Dull T, Mandel RJ, Bukovsky A, Quiroz D, Naldini L, et al. Self-inactivating lentivirus vector for safe and efficient in vivo gene delivery. J Virol. 1998;72:9873–80.
18. Hendel A, Bak RO, Clark JT, Kennedy AB, Ryan DE, Roy S, et al. Chemically modified guide RNAs enhance CRISPR-Cas genome editing in human primary cells. Nat Biotechnol. 2015;33:985–9.
19. Jedema I, Barge RM, Willemze R, Falkenburg JH. High susceptibility of human leukemic cells to Fas-induced apoptosis is restricted to G1 phase of the cell cycle and can be increased by interferon treatment. Leukemia. 2003;17:576–84.
20. Uy GL, Rettig MP, Motabi IH, McFarland K, Trinkaus KM, Hladnik LM, et al. A phase 1/2 study of chemosensitization with the CXCR4 antagonist plerixafor in relapsed or refractory acute myeloid leukemia. Blood. 2012;119:3917–24.
21. Rettig MP, Ritchey JK, Prior JL, Haug JS, Piwnica-Worms D, DiPersio JF. Kinetics of in vivo elimination of suicide gene-expressing T cells affects engraftment, graft-versus-host disease, and graft-versus-leukemia after allogeneic bone marrow transplantation. J Immunol. 2004;173:3620–30.
22. Gross S, Piwnica-Worms D. Real-time imaging of ligand-induced IKK activation in intact cells and in living mice. Nat Methods. 2005;2:607–14.
23. Tsai SQ, Zheng Z, Nguyen NT, Liebers M, Topkar VV, Thapar V, et al. GUIDE-seq enables genome-wide profiling of off-target cleavage by CRISPR-Cas nucleases. Nat Biotechnol. 2015;33:187–97.
24. Festing MF, Altman DG. Guidelines for the design and statistical analysis of experiments using laboratory animals. ILAR J. 2002;43:244–58.
25. Mead R. The Design of Experiments: Statistical Principles for Practical Applications. Cambridge: Cambridge University Press. 1988.
26. Eissenberg LG, Rettig MP, Ritchey JK, Prior JL, Schwarz SW, Frye J, et al. [18F]FHBG PET/CT imaging of CD34-TK75 transduced donor T cells in relapsed allogeneic stem cell transplant patients: safety and feasibility. Mol Ther. 2015;23:1110–22.
27. Png YT, Vinanica N, Kamiya T, Shimasaki N, Coustan-Smith E, Campana D. Blockade of CD7 expression in T cells for effective chimeric antigen receptor targeting of T-cell malignancies. Blood Adv. 2017;1:2348–60.
28. Gomes-Silva D, Srinivasan M, Sharma S, Lee CM, Wagner DL, Davis TH, et al. CD7-edited T cells expressing a CD7-specific CAR for the therapy of T-cell malignancies. Blood. 2017;130:285–96.
29. Mamonkin M, Rouce RH, Tashiro H, Brenner MK. A T-cell-directed chimeric antigen receptor for the selective treatment of T-cell malignancies. Blood. 2015;126:983–92.
30. Osborn MJ, Webber BR, Knipping F, Lonetree CL, Tennis N, DeFeo AP, et al. Evaluation of TCR gene editing achieved by TALENs, CRISPR/Cas9, and megaTAL nucleases. Mol Ther. 2016;24:570–81.
31. Qasim W, Zhan H, Samarasinghe S, Adams S, Amrolia P, Stafford S, et al. Molecular remission of infant B-ALL after infusion of universal TALEN gene-edited CAR T cells. Sci Transl Med. 2017;9:eaaj2013.
32. Pinz K, Liu H, Golightly M, Jares A, Lan F, Zieve GW, et al. Preclinical targeting of human T-cell malignancies using CD4-specific chimeric antigen receptor (CAR)-engineered T cells. Leukemia. 2016;30:701–7.
33. Tiftik N, Bolaman Z, Batun S, Ayyildiz O, Isikdogan A, Kadikoylu G, et al. The importance of CD7 and CD56 antigens in acute leukaemias. Int J Clin Pract. 2004;58:149–52.

34. Miwa H, Nakase K, Kita K. Biological characteristics of CD7(+) acute leukemia. Leuk Lymphoma. 1996;21:239–44.
35. Bonilla FA, Kokron CM, Swinton P, Geha RS. Targeted gene disruption of murine CD7. Int Immunol. 1997;9:1875–83.
36. Reinhold U, Liu L, Sesterhenn J, Abken H. CD7-negative T cells represent a separate differentiation pathway in a subset of post-thymic helper T cells. Immunology. 1996;89:391–6.
37. Stock W, Sanford B, Lozanski G, Vij R, Byrd JC, Powell BL, et al. Alemtuzumab can be incorporated into front-line therapy of adult acute lymphoblastic leukemia (ALL): final phase I results of a Cancer and Leukemia Group B Study (CALGB 10102). Blood. 2009;114:345–345.
38. Gökbuget N, Basara N, Baurmann H, Beck J, Brüggemann M, Diedrich H, et al. High single-drug activity of nelarabine in relapsed T-lymphoblastic leukemia/lymphoma offers curative option with subsequent stem cell transplantation. Blood. 2011;118:3504–11.
39. Kleinstiver BP, Pattanayak V, Prew MS, Tsai SQ, Nguyen NT, Zheng Z, et al. High-fidelity CRISPR-Cas9 nucleases with no detectable genome-wide off-target effects. Nature. 2016;529:490–5.
40. Eyquem J, Mansilla-Soto J, Giavridis T, van der Stegen SJC, Hamieh M, Cunanan KM, et al. Targeting a CAR to the TRAC locus with CRISPR/Cas9 enhances tumour rejection. Nature. 2017;543:113–7.
41. MacLeod DT, Antony J, Martin AJ, Moser RJ, Hekele A, Wetzel KJ, et al. Integration of a CD19 CAR into the TCR alpha chain locus streamlines production of allogeneic gene-edited CAR T cells. Mol Ther. 2017;25:949–61.
42. Cooke KR, Kobzik L, Martin TR, Brewer J, Delmonte J Jr, Crawford JM, et al. An experimental model of idiopathic pneumonia syndrome after bone marrow transplantation: I. The roles of minor H antigens and endotoxin. Blood. 1996;8:3230–9.